PERGAMON

Acta mater. 48 (2000) 2339–2347

Acta MATERIALIA

www.elsevier.com/locate/actamat

DEFECT STRUCTURES IN $ZrCo_2$ LAVES PHASE

J. H. ZHU† and C. T. LIU

Oak Ridge National Laboratory, Metals and Ceramics Division, Bldg. 4500S-MS6115, PO Box 2008, Oak Ridge, TN 37831-6115, USA

(Received 6 December 1999; accepted 27 December 1999)

Abstract—Point defect structures in the C15 $ZrCo_2$ alloys were studied by bulk density and X-ray lattice parameter measurements. It was found that, for the $ZrCo_2$ alloys quenched from 1000°C, the lattice parameter increases linearly as the Zr content increases up to 33.3 at.% Zr. The lattice parameter of the Laves phase remains constant for the alloys with Zr content higher than 33.3 at.%, indicating that the solubility range of Zr in $ZrCo_2$ on the Zr-rich side is essentially zero. The constitutional defects were found to be of the anti-site type. Thermal vacancies exhibiting a maximum at the stoichiometric composition were observed in the $ZrCo_2$ Laves phase alloys after quenching from 1250 and 1000°C, with higher thermal vacancies obtained from 1250°C. The defect structures in the $ZrCo_2$ phase may be correlated to the relative magnitude of formation enthalpies for anti-site and quadruple defects in this compound. Thermal vacancy concentration at a level of 1% in $ZrCo_2$ does not affect fracture toughness at room temperature. *Published by Elsevier Science Ltd on behalf of Acta Metallurgica Inc.*

Keywords: Intermetallic compound; Casting; X-ray diffraction; Lattice defects; Mechanical properties (fracture & fracture toughness)

1. INTRODUCTION

Topologically close packed Laves phases with AB_2 composition are known to be size compounds, i.e., the atomic size ratio, R_A/R_B, is ideally 1.225, with a range of 1.05–1.67 typically observed [1, 2]. Laves phases are conventionally considered to be line compounds with a strict AB_2 composition. However, about 25% of the binary Laves phases show certain homogeneity ranges on the A- and/or B-rich side of stoichiometry [3]. Non-stoichiometric intermetallic compounds are stabilized by the incorporation of constitutional defects. The excess atoms in off-stoichiometric compounds may prefer to (1) stay on their own sublattice, leading to the formation of constitutional vacancies on the other sublattice, (2) insert into interstitial sites, or (3) occupy the sites on the other sublattice, leading to the formation of substitutional anti-site defects. Since Laves phases have topologically close packed (TCP) structures and space-filling is relatively high, there are no interstitial sites with a size comparable to that of the component atoms. Therefore, the insertion of the excess atoms into the interstitial sites can be excluded, and the possible defect mechanisms in binary Laves phases are thus constitutional vacancy or anti-site substitution.

The defect structures in cubic C15 $NbCr_2$, $NbCo_2$ and hexagonal C14 $NbFe_2$ Laves phases have recently been determined to be of anti-site type on both sides of stoichiometry [4]. Contrary to the geometric considerations which support the constitutional vacancy mechanism on the A-rich side of stoichiometry, anti-site substitution is found to be the constitutional defect mechanism on the Nb-rich side of these Laves phases. These results indicate that except for the geometric factor, other factors such as chemical bonding characteristics may also affect the defect structures in this Laves phases. Based on geometric and thermodynamic considerations, Laves phases with atomic size ratio R_A/R_B larger than 1.225 and/or high negative enthalpy of formation (ΔH) may exhibit constitutional vacancies in the A-rich side, as suggested by Zhu *et al.* [4].

By heating the ordered Laves phases, thermal defects can also be created in the compounds. Modder and his coworkers [5, 6] have systematically analyzed the possible defect type in Laves phases and two types of thermal defects were identified, namely quadruple defects (consisting of one anti-site B atom on the A-atom sublattice and three

† To whom all correspondence should be addressed.

1359-6454/00/$20.00 Published by Elsevier Science Ltd on behalf of Acta Metallurgica Inc.
PII: S1359-6454(00)00014-8

vacancies on the B-atom sublattice) and anti-site defects. Furthermore, it was found that the defect types in Laves phases can be correlated to the relative magnitudes of the formation enthalpies of anti-site and quadruple defects in the compounds [6].

The point defect structures in the $ZrCo_2$ system have not been investigated previously. The atomic size ratio R_A/R_B of $ZrCo_2$ is 1.28, which is significantly larger than the ideal one, i.e., 1.225. Furthermore, the enthalpy of formation (ΔH) of $ZrCo_2$ is -113 kJ/mole [7], which is much more negative than those of $NbCr_2$, $NbCo_2$ and $NbFe_2$ Laves phases. So far, no work has been conducted to carefully determine the homogeneity range and defect structures in the Laves phase. The binary Co–Zr phase diagram shows certain solubilities on both sides of stoichiometry in this Laves phase system [8]. All these facts indicate that the $ZrCo_2$ Laves phase system deserves further attention as a system where constitutional vacancies may be the defect mechanism on the Zr-rich side.

In the present study, we have attempted to determine the solubility range and to model the defect structures in binary $ZrCo_2$ alloys with different stoichiometric compositions, by measuring the lattice parameters, bulk densities, and therefore, vacancy concentrations of binary $ZrCo_2$ alloys of various compositions after quenching from 1000 and 1250°C. Thermal defects that will be introduced by quenching from elevated temperatures have also been determined. The fracture toughness of selected alloys were also measured at room temperature.

2. EXPERIMENTAL PROCEDURES

The alloy compositions investigated in this study are listed in Table 1. A total of seven binary alloys were prepared. The Zr content in the alloy increases with the alloy code number. The alloys ♯1–♯3 are Co-rich and ♯4 is the stoichiometric alloy, while alloys ♯5–♯7 are Zr-rich. Ingots weighing approximately 50 g were prepared by arc-melting techniques using high-purity starting materials. Each ingot was remelted at least five times to ensure compositional homogeneity before being cast into a 12.7 mm diameter cylinder. The weight loss during arc-melting was essentially zero (less than 0.01 g). It should be noted that the ingots of the alloys ♯4–♯7 remained in one piece, while the ingots of the alloys ♯1–♯3 broke into several pieces after drop casting.

After a homogenization anneal at 1200°C for 20 h in vacuum, the alloys were encapsulated in quartz, which was then evacuated and backfilled with helium. The encapsulated alloys were then heat-treated at 1000°C for 7 days and water quenched. Small fractions of the quenched samples were mounted for microstructural observation using an optical microscope and for chemical composition analyses of the phases present using a field-emission-gun scanning electron microscope (SEM) equipped with an energy dispersive X-ray spectrometer (EDS). All the alloys were found to be fully homogenized following the above heat treatments.

The remaining parts of the samples were crushed in an agate mortar into powders with particle sizes smaller than 40 mesh. Powders with a mesh size of $-40+80$ were used for bulk density measurements, and powders smaller than 320 mesh were used for X-ray analyses. The bulk density was measured using a helium pycnometer with an accuracy of approximately 0.01 vol.%. Powdered samples were used to eliminate the micropores generated during solidification, which leads to more accurate density measurements. The vacancy concentration of the Laves-phase alloys, c_V, is defined as the ratio of the total number of vacancies to the total number of atoms. It can be obtained from the following equation:

$$c_V = \frac{\rho_X - \rho_B}{\rho_B} \tag{1}$$

where ρ_X and ρ_B are the X-ray and the bulk densities, respectively.

The powdered samples of the single-phase alloys ♯1–♯4 were then wrapped in Ta sheets and encapsulated in quartz, which was evacuated and backfilled with helium. They were then heat-treated at 1250°C for 2 h and water quenched. Bulk densities and lattice parameters were measured again and the

Table 1. Composition, lattice parameter, X-ray density, bulk density and vacancy concentration of $ZrCo_2$ alloys quenched from 1250 and 1000°C

Alloy code	Zr (at.%)	Lattice parameter (Å)		X-ray density (g/cm^3)		Bulk density (g/cm^3)		Vacancy concentration (%)	
		1250°C	1000°C	1250°C	1000°C	1250°C	1000°C	1250°C	1000°C
#1	30.8	6.9305	6.9311	8.242	8.240	8.194	8.224	0.58	0.20
#2	31.8	6.9419	6.9430	8.240	8.235	8.192	8.210	0.59	0.31
#3	32.8	6.9543	6.9546	8.234	8.233	8.177	8.203	0.70	0.37
#4	33.3	6.9590	6.9608	8.236	8.230	8.155	8.196	1.00	0.42
#5	33.5	–	6.9609[a]	–	–	–	–	–	–
#6	33.8	–	6.9607[a]	–	–	–	–	–	–
#7	34.3	–	6.9609[a]	–	–	–	–	–	–

[a] Two-phase alloys with the lattice parameter of the $ZrCo_2$ Laves phase listed here.

vacancy concentrations were obtained for these alloys quenched from 1250°C.

X-ray diffraction measurements were made using a Scintag XD2000 diffractometer with Cu K_α radiation. The lattice parameter was determined from 13–15 peaks. The X-ray density was calculated using the measured lattice parameter. The accuracy of the vacancy concentration using our method is approximately 0.08%, which is mainly due to the compositional uncertainty of the alloys.

The fracture toughness of the selected alloys was also determined using the indentation method with a load of 500 g and a holding time of 15 s. The crack lengths were measured immediately after the indentation to eliminate the possibility of slow crack propagation following the removal of the indenter. The following equation was used to calculate the fracture toughness of the alloys [9]:

$$K_{IC} = A\left[\frac{E}{H}\right]^n \frac{P}{L^{3/2}} \quad (2)$$

where K_{IC} is the fracture toughness (MPa$\sqrt{m}$), E is Young's modulus (GPa), which is assumed to be 218 GPa for all of the investigated alloys, H is Vickers hardness (GPa), P is the load (N), and L the average length of the four radial cracks from the center of the indent to the crack tip. A and n are constants, which are taken as 0.016 and 0.5, respectively, for relatively brittle materials [9].

3. RESULTS

3.1. Microstructure

Microstructure examinations of the $ZrCo_2$ Laves phase alloys listed in Table 1 after quenching from 1000°C indicate that alloys ♯1–♯4 are in the single-phase region, while alloys ♯5–♯7 are in the two-phase region. Typical microstructures of single-phase and two-phase alloys are shown in Figs 1(a) and (b). Note that Fig. 1(a) was taken from the Co–33.3%Zr sample (alloy ♯4) etched with a solution of 60% glycerine + 20% HNO_3 + 10% HF + 10% H_2O (in vol.%), while Fig. 1(b) was from the Co–34.3%Zr sample (alloy ♯7) in the as-polished condition under polarized light. There are no annealing twins in the alloys, unlike the $NbCr_2$ system [4], indicating relatively high stacking fault energy in this compound. The second phase in alloys ♯5–♯7 was analyzed with EDS in an SEM, and was found to be richer in Zr than the $ZrCo_2$ matrix. According to the binary Co–Zr phase diagram [8], this second phase is a ζ phase with a B2 structure. The maximum content of Zr in $ZrCo_2$ at 1000°C is found to be about 33.3 at.% from this study, which is different from the estimated phase boundary in the binary Co–Zr phase diagram [8, 10], where it was indicated to be about 34.5 at.%. Furthermore, extensive cracking was observed in the matrix around the second phase. These cracks are most likely caused by the thermal residual stress in the alloys after casting and heat treatment, as a result of the mismatch in thermal expansion coefficients between the second phase and the matrix.

3.2. Lattice parameter, density, and vacancy concentration

The lattice parameters of the C15 $ZrCo_2$ alloys listed in Table 1 are plotted in Fig. 2 as a function of stoichiometry for all the samples quenched from 1000°C and for the single-phase alloys quenched from 1250°C. As the Zr content increases, the lattice parameter of the $ZrCo_2$ phase also increases. For the Co-rich alloys quenched from 1250 and 1000°C, the data points fit nicely along two straight lines, while on the Zr-rich side the lattice constants are identical for alloys ♯5–♯7 quenched from

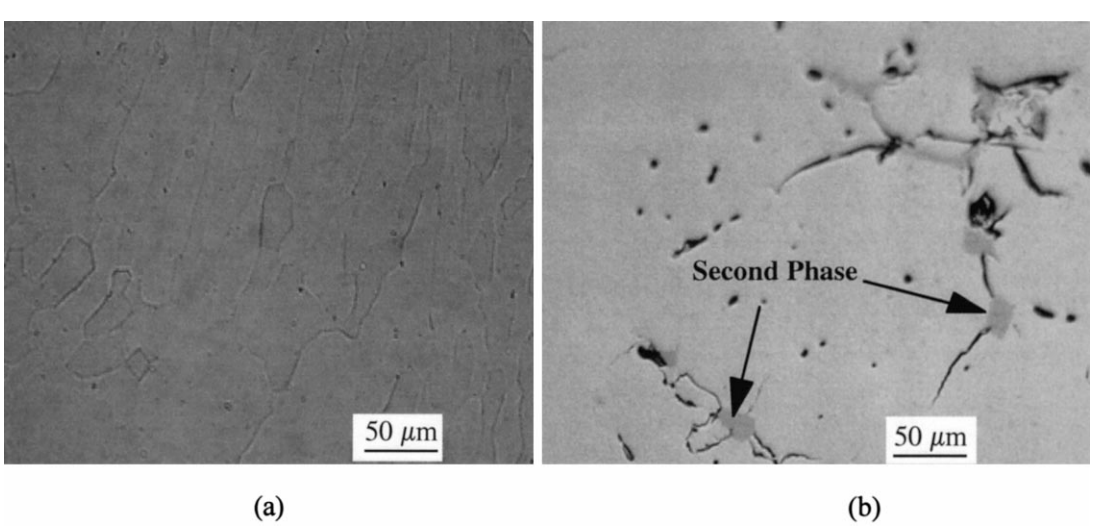

Fig. 1. Optical micrographs of $ZrCo_2$ alloys: (a) alloy ♯4, etched; (b) alloy ♯7, as-polished.

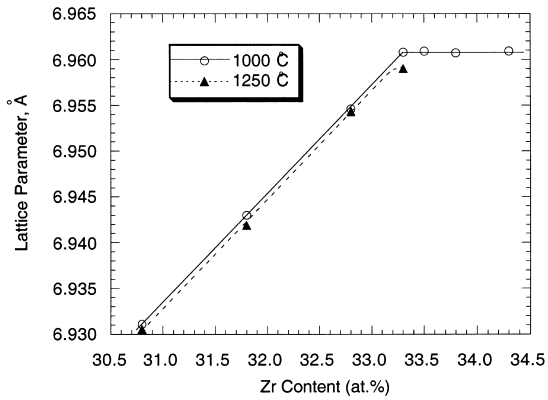

Fig. 2. Lattice parameter as a function of Zr content after quenching from 1250 and 1000°C.

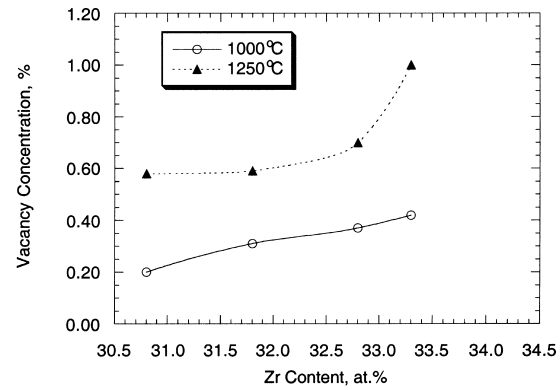

Fig. 4. Vacancy concentration as a function of Zr content after quenching from 1250 and 1000°C.

1000°C, indicating that the composition of the Laves phase is the same in the alloys with more than 33.3% Zr (see Fig. 2). This is expected, because the maximum content of Zr in $ZrCo_2$ is about 33.3 at.% and these three alloys were found to be in the two-phase region. The lattice parameters after quenching from 1250°C are a little bit smaller, compared to those after quenching from 1000°C. This can be due to the presence of vacancies in the alloy.

The X-ray and bulk density results for alloys ♯1–♯4 after quenching from both 1250 and 1000°C are presented in Table 1 and Fig. 3. The density of the alloys decreases as the Zr content increases, and the bulk density after quenching from 1000°C is consistently higher than those after quenching from 1250°C. Using equation (1) and the data presented in Table 1 and Fig. 3, the vacancy concentrations were calculated, and are listed in Table 1. Due to the presence of the second phase, the vacancy concentration could not be determined for alloys ♯5–♯7. Figure 4 is a plot of the vacancy concentration as a function of the Zr content for the single-phase $ZrCo_2$ alloys after quenching from the two different temperatures. It is noted that the vacancy concentration is quite high after quenching from 1250°C. The vacancy concentration reaches a maximum of ~1.0% at the stoichiometric composition and decreases on the Co-rich side of stoichiometry. Annealing and quenching from 1000°C results in vacancy concentrations lower than those after quenching from 1250°C. However, a maximum at the stoichiometric composition can also be recognized.

3.3. Fracture toughness

The fracture toughness values of the single-phase $ZrCo_2$ alloys after quenching from 1000°C were measured as a function of Zr content (see Fig. 5). It was found that all the single-phase $ZrCo_2$ alloys exhibit a fracture toughness value of around 1 MPa

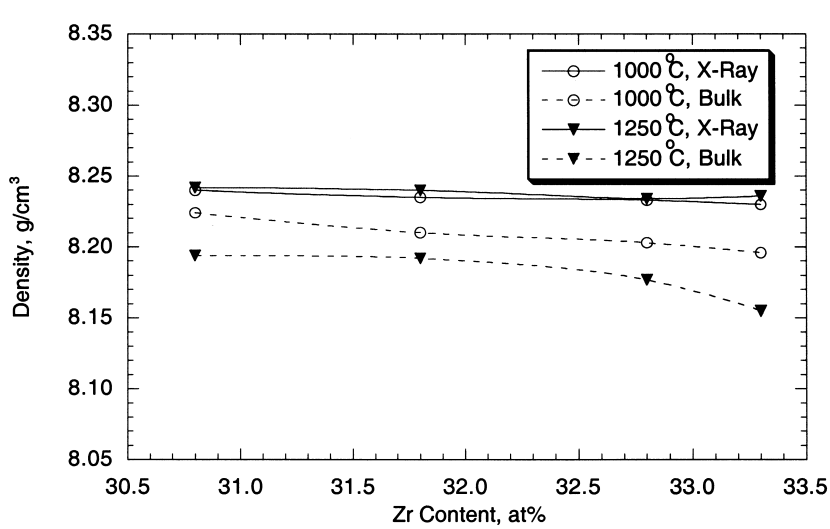

Fig. 3. X-ray and bulk densities as a function of Zr content after quenching from 1250 and 1000°C.

$m^{1/2}$, regardless of the alloy stoichiometry. Furthermore, the fracture toughness value of the stoichiometric $ZrCo_2$ alloy after quenching from 1250°C was found to be close to that of the same alloy after quenching from 1000°C, even though the vacancy concentration in the alloy is much higher after quenching from 1250°C. This indicates that the presence of such vacancies does not lead to toughness improvement in this Laves phase.

4. DISCUSSION

4.1. Constitutional defect mechanisms in $ZrCo_2$ Laves phase

The vacancy concentration as a function of stoichiometry for binary Laves phases has been calculated based on the two constitutional defect models, i.e., the constitutional vacancy model and anti-site substitution model [4]. The constitutional vacancy model is based on the assumption that all the excess atoms exclusively stay on their own sublattice, thus constitutional vacancies are created on the sublattice of the other element. Based on this model, the constitutional vacancy concentrations in Laves phases are zero at the stoichiometric composition and increase on both sides of stoichiometry. The anti-site substitutional model assumes that the excess atoms occupy the sublattice sites of the other species. Thus, anti-site defects are created, and no constitutional vacancies are needed for the balance of the lattice sites. The constitutional vacancy concentrations are zero for both A- and B-rich Laves phases, according to the anti-site substitutional model.

From Fig. 4, it is obvious that the measured vacancy concentrations for all the single-phase $ZrCo_2$ alloys after quenching from 1000°C are relatively low (see also Table 1), indicating that there are no constitutional vacancies in these Laves phases. Furthermore, as the composition deviates further from the stoichiometry, the vacancy concentration on the Co-rich side decreases, while the constitutional vacancy model predicts an opposite trend. Actually, the measured vacancy concentration as a function of stoichiometry can be rationalized by assuming that these vacancies are thermal vacancies instead of constitutional vacancies (see next section for more details). This is consistent with the anti-site substitution model and contrary to the constitutional vacancy model, which demands much higher vacancy concentrations for off-stoichiometric compositions. Thus, the constitutional defects are of anti-site type for the Co-rich $ZrCo_2$ Laves phases.

Point defect mechanisms in binary Laves phases have been the focus of several studies. Fleischer [11] found that anti-site substitution occurs on both sides of stoichiometry for the C15 $ZrCr_2$ Laves phase. Pargeter and Hume-Rothery [12] and Saito and Beck [13] investigated the point defects in Co-rich $NbCo_2$ and dihexagonal C36 $NbCo_3$ Laves phases and found that in both phases, the deviation from stoichiometry resulted from the substitution of Co atoms for the Nb atoms. X-ray and neutron diffraction measurements [14] showed that for both $ZrFe_2$ and $TiFe_2$, the excess Fe atoms are on the Zr or Ti sublattice. The constitutional defect structure of the $NbFe_2$ Laves phase was also investigated by measuring the lattice parameters on both sides of stoichiometry, and again anti-site substitution was found to be the defect mechanism [15]. YAl_2 Laves phase is a line compound with negligible solubility existing under equilibrium conditions; however, Foley *et al.* extended the solubility on both sides of stoichiometry in this alloy system via rapid solidification. From lattice parameter measurements, off-stoichiometry in the YAl_2 Laves phase was postulated to be accompanied by different defect mechan-

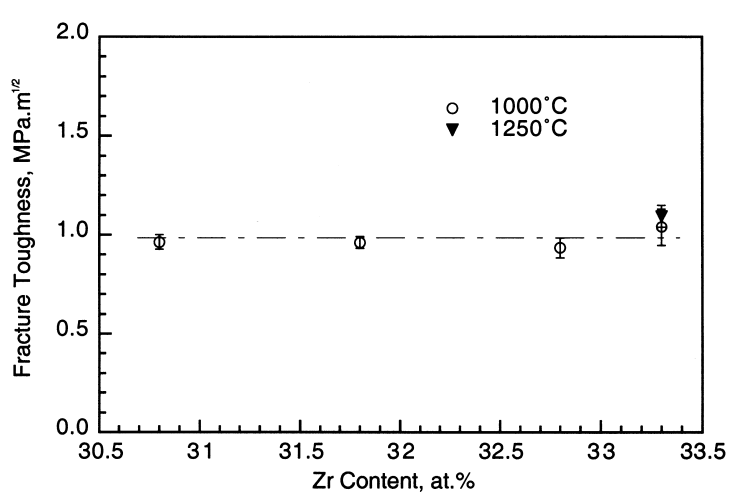

Fig. 5. Fracture toughness vs Zr content for $ZrCo_2$ alloys after quenching from 1250 and 1000°C.

isms: the Y-rich side is accommodated by vacancies, while the Al-rich compositions result from anti-site substitution [16]. Recent studies combining bulk density and X-ray lattice parameter measurements unambiguously indicate that the constitutional defect mechanisms in binary C15 $NbCr_2$, $NbCo_2$, and C14 $NbFe_2$ compounds on both sides of stoichiometry are of anti-site type, with no constitutional vacancies present in the compounds [4].

Table 2 summarizes the atomic size ratio R_A/R_B, enthalpy of formation and point defect structures for a number of binary Laves phases [17]. Based on geometric considerations, the atomic size ratio R_A/R_B of the AB_2 Laves phases should be important in controlling the point defect structures in Laves phases. For Laves phases with R_A/R_B greater than the ideal ratio of 1.225, on the A-rich side, it will be more difficult for A atoms to stay on the sublattice sites of B atoms as the atomic size ratio increases. Therefore, it would be possible to obtain constitutional vacancies for Laves phases with $R_A/R_B > 1.225$ on the A-rich side, even though substitutional anti-site defects are most likely to form under all the other circumstances. In all the AB_2 Laves phases whose point defect structure on the A-rich side has been studied so far and listed in Table 2, only YAl_2 has an R_A/R_B ratio of 1.258, higher than the ideal one, and this alloy system also shows certain indications of constitutional vacancies in the Y-rich compounds [16]. For the $ZrFe_2$ alloys with the R_A/R_B ratio of 1.257, the defect structure on the Zr-rich side has not been studied yet. For the $ZrCo_2$ compound, R_A/R_B is 1.280, much larger than the ideal. Therefore, the possibility is expected to be higher for constitutional vacancies existing in this system.

On the other hand, Neumann [18] found that for B2 compounds their constitutional defect structure is closely related to the magnitude of enthalpy of formation. Constitutional vacancies are the preferred defect mechanism for B2 compounds that are more strongly ordered with more negative enthalpy of formation (ΔH) values on the large atom-rich side of stoichiometry, while B2 compounds with ΔH higher than −75 to −90 kJ/mole generally exhibit the anti-site defect structure. Similar thermodynamic arguments may hold for binary Laves phases. As listed in Table 2, anti-site defects are observed on the large atom-rich side for those Laves phases with ΔH value higher than −75 to −90 kJ/mole such as $NbCr_2$, $NbCo_2$, and $NbFe_2$. For Laves phases with more negative ΔH values, such as YAl_2 with a ΔH value of −160.4 kJ/mole [17], constitutional vacancies are the possible defect mechanism on the Y-rich side. In this regard, $ZrCo_2$ also has a highly negative ΔH value of −123 kJ/mole, and thus constitutional vacancies may form on the Zr-rich side.

Based on both geometric and thermodynamic considerations, therefore, constitutional vacancies may be created on the Zr-rich side of $ZrCo_2$, similar to the case of YAl_2. Unfortunately, this study indicates that the solubility range of Zr is essentially zero in $ZrCo_2$ on the Zr-rich side, which makes it difficult to verify our hypothesis regarding the effects of atomic size ratio and enthalpy of formation on the defect mechanisms in binary Laves phases. Rapid solidification techniques could be utilized in future investigations to extend the solubility range on the Zr-rich side in this compound and defect structures can then be deduced from the lattice parameter measurement, as in the case of the YAl_2 phase [16]. It would also be interesting to study defect structures in other Laves phases with $R_A/R_B > 1.225$ and/or highly negative enthalpy of formation to consider whether it is possible to introduce constitutional vacancies on the A-rich side in these compounds.

The fact that both YAl_2 and $ZrCo_2$ compounds are unstable on the A-rich side of stoichiometry under equilibrium conditions indicates that the creation of constitutional vacancies may make the compound energetically less stable. This may explain the lack of solubility on the A-rich side of these compounds. Furthermore, anti-site defects may also be impossible to form on the A-rich side in these compounds, due to the difficulties involved in A-atoms occupying the much smaller B-atom sublattice sites. Consequently, it may be impossible or at least very difficult to obtain constitutional defects in these Laves phases.

4.2. Thermal defects in $ZrCo_2$ Laves phase

As Modder and Bakker have pointed out, it is very possible that a vacancy-type defect termed

Table 2. Atomic size ratio, enthalpy of formation and point defect structure of a number of binary Laves phases

Compound	R_A/R_B[a]	ΔH (kJ/mole)[a]	Defect structure
$NbCr_2$	1.145	−21	Anti-site substitution on both sides
$NbCo_2$	1.173	−51	Anti-site substitution on both sides
$NbFe_2$	1.152	−62	Anti-site substitution on both sides
$ZrFe_2$	1.257	−75	Fe-rich side: anti-site substitution
$TiFe_2$	1.148	−84	Fe-rich side: anti-site substitution
YAl_2	1.258	−160.4	Al-rich side: anti-site substitution Y-rich side: constitutional vacancy
$ZrCo_2$	1.280	−123	Co-rich side: anti-site substitution Zr-rich side: unknown

[a] The R_A/R_B and ΔH values for these compounds are from Ref. [17].

quadruple defect occurs in C15 compounds [5]. Furthermore, ball milling was found to introduce quadruple defects in $GdAl_2$, $GdPt_2$, $GdIr_2$ and $GdRh_2$, while anti-site defects were created in $GdMg_2$ [6]. Since ball milling usually leads to the formation of the same type of atomic defects as heating, thermal defects such as quadruple defects or anti-site defects may be created upon quenching the Laves phases from elevated temperatures. Since each quadruple defect contains three vacancies, thermal vacancies are expected if quadruple defects are created.

The vacancy concentrations in $ZrCo_2$ alloys are quite high after quenching from 1250°C and the vacancy concentrations are significantly reduced after annealing at lower temperature, i.e., 1000°C (Fig. 4). Since the constitutional defects in this compound have been established to be of the anti-site type, these vacancies are obviously thermal vacancies. The fact that the vacancy concentration increases as the quenching temperature increases is a further indication of the thermal nature of these vacancies. Thus, the quadruple defects may be formed in this compound by heating. According to the quadruple defect model and considering the difficulties involved in Zr sitting on the small atom Co sites, Co will go to the Zr sublattice and thus the thermal vacancies are on the Co sublattice sites. Furthermore, the measured vacancy concentration reaches a peak at the stoichiometric composition and decreases on deviating from stoichiometry for the $ZrCo_2$ alloys when quenched from 1250°C and 1000°C (Fig. 4). This behavior is similar to the $NbCr_2$ system [9], where the thermal vacancy concentration exhibits a maximum at the stoichiometric composition. As in the $NbCr_2$ phase, a maximum in thermal vacancy concentration at the stoichiometric composition is rationalized by considering that the increase in entropy associated with the introduction of vacancies will be the greatest at the stoichiometric composition, where the degree of order is necessarily the highest.

Modder *et al.* [6] have extended Miedema's model to estimate the formation enthalpy of quadruple and anti-site defects in C15 Laves phases. According to this model, the type of atomic disorder is related to the relative magnitudes of formation enthalpies of anti-site and quadruple-defect disorder for the Laves phases. Therefore, the presence of thermal vacancies in $ZrCo_2$ may imply that the formation enthalpies of anti-site disorder is larger in magnitude than that of quadruple defect disorder for $ZrCo_2$. Furthermore, the higher vacancy concentration of $ZrCo_2$ after quenching, compared to $NbCr_2$, suggests that the formation enthalpy of quadruple defects in $ZrCo_2$ should be lower than that in $NbCr_2$, which leads to a higher amount of thermal defects in $ZrCo_2$ phase.

It has been suggested that vacancies in Laves phases may assist the synchroshear deformation mechanism and thus increase the toughness of the Laves alloys [19]. Even though thermal vacancies are relatively high (~1%) in the $ZrCo_2$ alloy after quenching from 1250°C, it was found that such quenched-in thermal vacancies do not affect the fracture toughness of the alloy. It will be of interest to determine the effect of constitutional vacancies on crack propagation and fracture toughness behavior of Laves phases if certain Laves phases with constitutional vacancies can be identified.

4.3. Reconstruction of the binary Co–Zr phase diagram

The existing Co–Zr phase diagram determined around 1964 by Pechin *et al.* [10] has not been updated so far. Those authors found that a homogeneity range of 28.4–34.6 at.% Zr exists for the $ZrCo_2$ Laves phase after rapidly quenching from 1400°C. In other words, there is 1.3 at.% Zr solubility on the Zr-rich side. Based on the present study, the solubility of Zr on the Zr-rich side is zero at 1000°C. This discrepancy may possibly be a result of the high impurity level in the materials used in the study by Pechin *et al.*, since they used the powder metallurgy (PM) method to produce the Laves phases, while in our study the arc-melting technique was employed. It is well known that impurities such as oxygen can easily be picked up during PM processing. The reaction of oxygen with Zr and the formation of ZrO_2 lower the Zr concentration in the Laves phase. Indeed, many voids and impurity particles (possibly ZrO_2) could be observed in the micrograph of the PM Laves phases [10]. Another possibility for the discrepancy may result from the fact that the quenching temperature is different for the two studies, with a much higher quenching temperature (1400°C) used in Pechin's study compared to 1000°C in the present study. The higher equilibrium temperature may increase the solubility range on the Zr-rich side of the compound.

In our view, this discrepancy is most likely due to the inaccurate composition control in Pechin *et al.*'s study, as is clear from the following argument. The slope of the lattice parameter as a function of stoichiometry for the Laves phase should usually change at the stoichiometric composition, as has been commonly observed for other Laves phases (for example, see Ref. [4]). According to Pechin *et al.* [10], the slope of the lattice parameter is the same on both sides of stoichiometry for $ZrCo_2$, suggesting that all the alloy compositions they prepared could be on one (Co-rich) side of stoichiometry, as a result of problems in material processing such as impurity pick-up. As has been demonstrated in the present study for the alloys quenched at 1000°C, negligible Zr solubility is observed for this Laves phase. Based on these arguments, we have refined the binary Co–Zr phase dia-

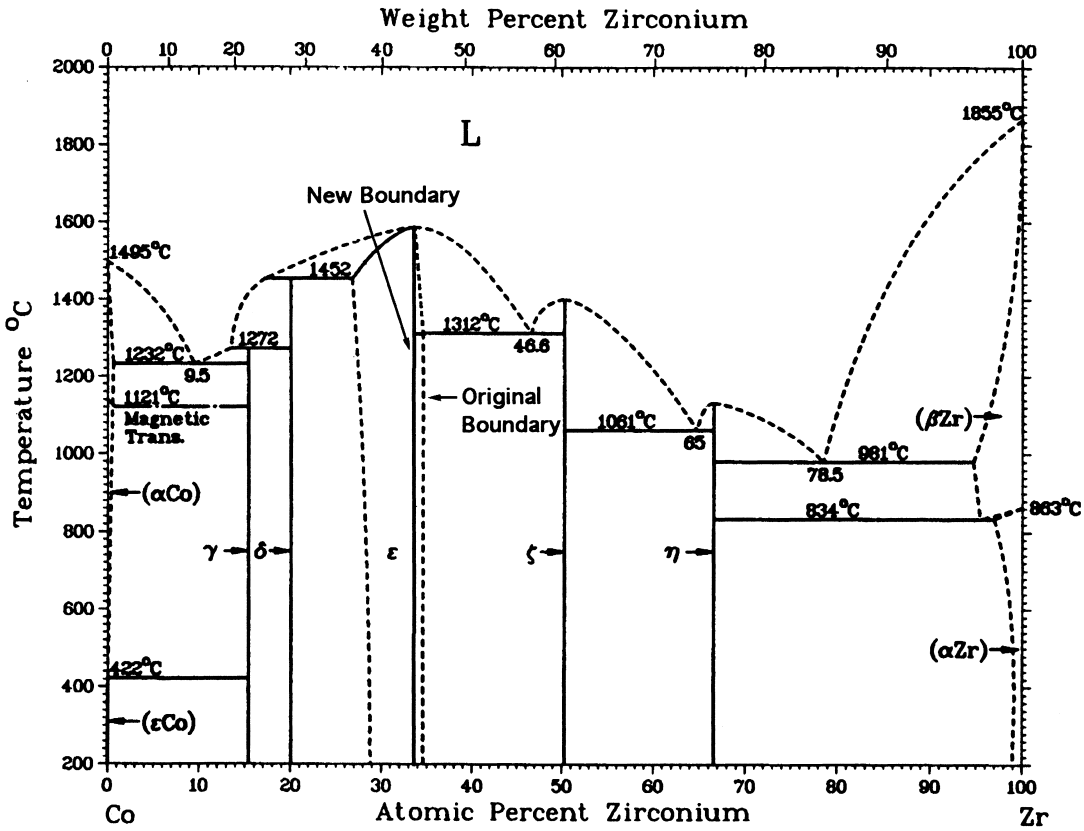

Fig. 6. The modified binary Co–Zr phase diagram.

gram, as shown in Fig. 6, where the solubility range of the Laves phase $ZrCo_2$ has been modified according to this study.

5. CONCLUSIONS

Point defects in the binary $ZrCo_2$ alloys have been clarified, combining both bulk density and X-ray lattice parameter measurements. The constitutional defects on the Co-rich side of stoichiometry for this system are of the anti-site type. As the Zr content in the Laves phase increases, the lattice parameters on the Co-rich side increase. The maximum content of Zr in the $ZrCo_2$ compound is the stoichiometric composition, 33.3 at.%. The binary Co–Zr phase diagram has been modified accordingly.

Thermal vacancies exhibiting a maximum at the stoichiometric composition were noted in $ZrCo_2$ Laves phase alloys after quenching from both 1000 and 1250°C, indicating that quadruple defects may be the type of thermal disorder in this compound. These thermal vacancies do not affect the fracture toughness of the Laves phase.

Acknowledgements—This research was sponsored by the Division of Materials Sciences, U.S. Department of Energy, under contract DE-AC05-96OR22464 with Lockheed Martin Energy Research Corporation. This research was supported in part by an appointment of J. H. Zhu to the Oak Ridge National Laboratory Postdoctoral Research Associates Program administered jointly by the Oak Ridge Institute for Science and Education and Oak Ridge National Laboratory (ORNL). Thanks are also due to S. R. Agnew and C. G. McKamey of ORNL for reviewing this manuscript.

REFERENCES

1. Laves, F., in *Theory of Alloy Phases*. American Society for Metals, Metals Park, OH, 1956, p. 124.
2. Zhu, J. H., Liu, C. T., Pike, L. M. and Liaw, L. M., *Metall. Mater. Trans.*, 1999, **30A**, 1449.
3. Thoma, D. J. and Perepezko, J. H., *J. Alloys Compounds*, 1995, **224**, 330.
4. Zhu, J. H., Pike, L. M., Liu, C. T. and Liaw, L. M., *Acta mater.*, 1999, **47**, 2003.
5. Modder, I. W. and Bakker, H., *Phys. Stat. Sol. (b)*, 1997, **199**, 369.
6. Modder, I. W., Kuin, M. J. and Bakker, H., *Intermetallics*, 1998, **6**, 537.
7. Klein, R., O'Hare, P. A. G. and Jacob, I., *J. Alloys Compounds*, 1997, **261**, 204.
8. Massalski, T. B., Murray, J. L., Bennett, L. H. and Baker, H., *Binary Alloy Phase Diagrams*. American Society for Metals, Metals Park, OH, 1986.
9. Sakai, M. and Bradt, R. C., *Int. Mater. Rev.*, 1993, **38**(2), 53.

10. Pechin, W. H., Williams, D. E. and Larsen, W. L., *Trans. ASM*, 1964, **57**, 464.
11. Fleischer, R. L., *Scripta metall. mater.*, 1992, **27**, 799.
12. Pargeter, J. K. and Hume-Ruthery, W., *J. Less-Common Metals*, 1967, **12**, 366.
13. Saito, S. and Beck, P. A., *Trans. Metall. Soc. AIME*, 1960, **218**, 670.
14. Brückner, W., Kleinstück, K. and Schulze, G. E. R., *Phys. Stat. Sol.*, 1967, **23**, 475.
15. Smith, A. W., Rogers, J. A. and Rawlings, R. D., *Phys. Stat. Sol. (a)*, 1973, **15**, K119.
16. Foley, J. C., Thoma, D. J. and Perepezko, J. H., *Metall. Trans.*, 1994, **25A**, 230.
17. Zhu, J. H., Metallurgical factors controlling the phase stability and mechanical behavior of transition-metal Laves phase alloy system. Ph.D. Dissertation, University of Tennessee, Knoxville, TN, August, 1998.
18. Neumann, J. P., *Acta metall.*, 1980, **28**, 1165.
19. Hazzledine, P. M. and Pirouz, P., *Scripta metall. mater.*, 1993, **28**, 1277.